

Camera characterization for thermal imaging quality control for silicon staves of the ATLAS phase II upgrade

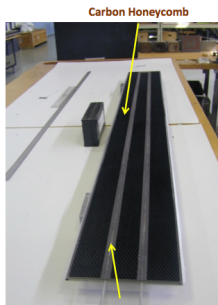
APS April Meeting 2016
Salt Lake City, Utah

Carlos Miguel Vergel-Infante ¹
Iowa State University, ATLAS Collaboration

¹cmvergel@iastate.edu

April 18, 2016



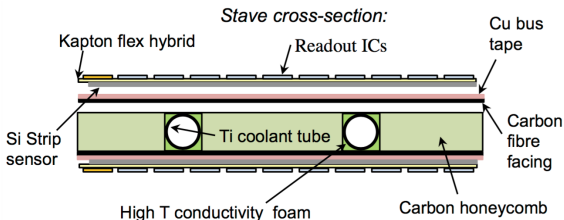


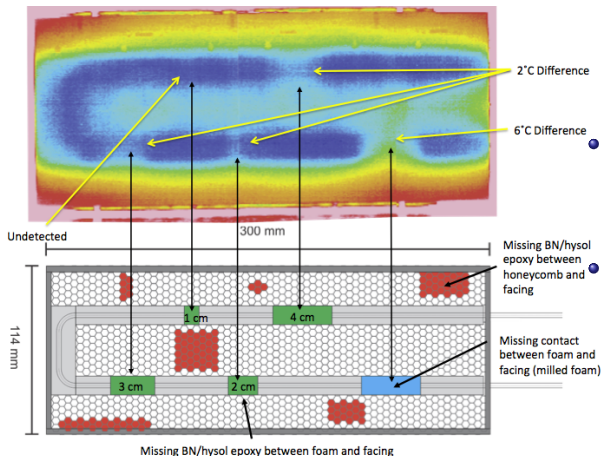
Pipe embedded in thermally conductive carbon foam



Kapton power/signal cable cured into carbon fiber facing

- Phase II upgrade of the ATLAS inner tracker (ITk) is under development. Expected in 2022.
- Staves serve as mechanical support for the strip sensors and readout modules, and to remove the dissipated heat out of the detector.
- A **Quality Control (QC)** test to detect any delaminations between the facing and the foam is required.

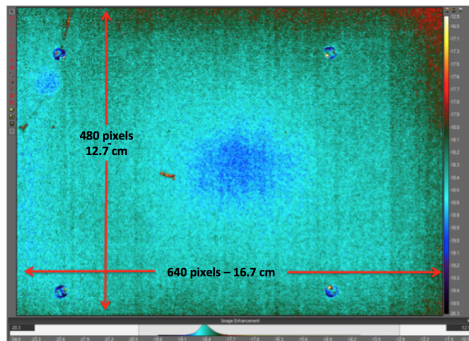




Test plate with flaws. Pipe's coolant at -30°C .

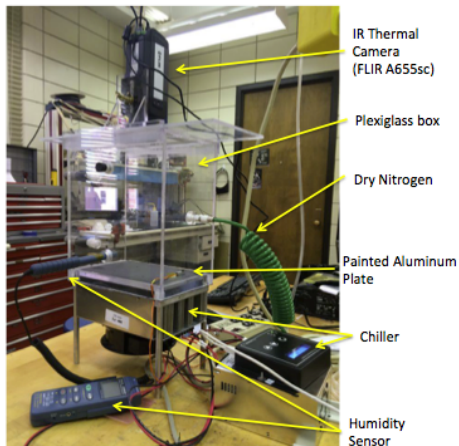
- The stave is inspected by an infrared (IR) thermal camera when its coolant pipe is cooled to around -40°C at ambient temperature.
- IR thermal imaging is mostly sensitive to **delaminations** between the **facing** and the **foam**.
- A good understanding of the thermal camera and its noise is necessary to optimize the detection of flaws with high sensitivity.

Experiment at ISU



Camera's Field of View (FoV) at -15°C .

- A painted aluminum plate is used to test the camera.
- The distance between camera and plate is 37.8 cm



Setup at ISU.



For a surface of constant temperature T a frame j obtained with the IR camera consists of sensors i readings of temperature raw values given by

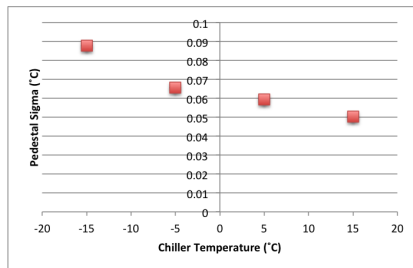
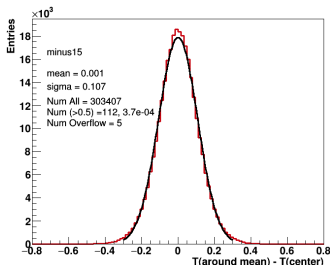
$$R_i^j = T + P_i + C^j + N_i^j + \Delta T_i.$$

- R_i^j Reading from the camera.
- T Real object's temperature.
- P_i Pedestal, pixel-by-pixel offset.
- C^j Common mode.
- N_i^j Statistical noise.
- ΔT_i External noise from the hardware of the camera as vignetting (lens).

Terms depend on object and ambient temperature.



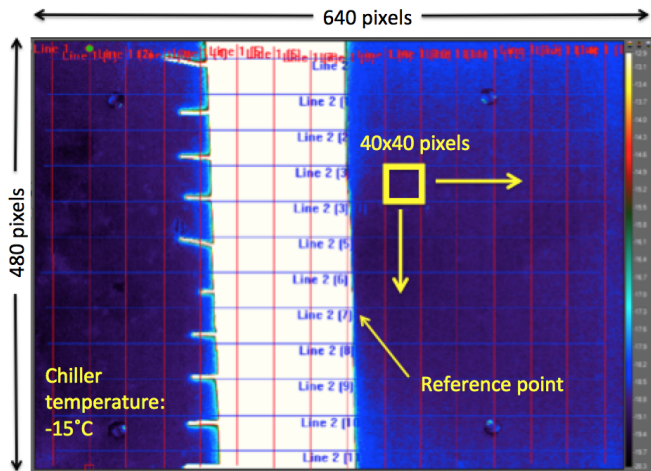
- Pedestal can be calculated for each pixel.
- The RMS of the pedestal (σ_P) shows the uniformity in the sensor readings.



- When the plate is cooled down at -15°C , the RMS of the pedestal is 0.11°C .
- σ_P increases when the plate's temperature decreases.

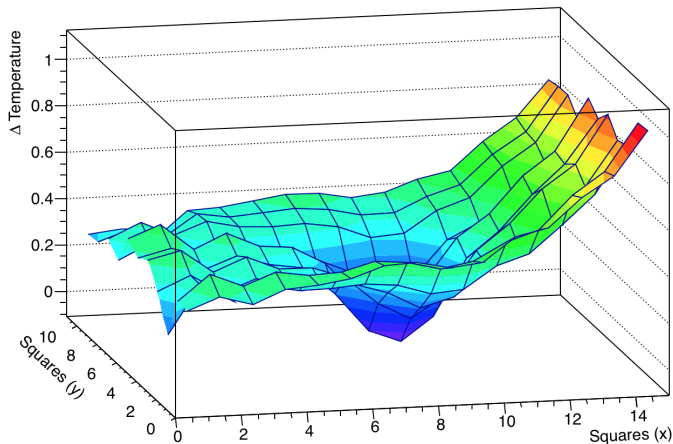
Vignetting

- Misreading in the object's temperatures at the edges of the lens.
- Scan the same physical square across the entire FoV.
- All squares should read the same except if there is vignetting.



Vignetting Shape

After mapping all the squares, this is the vignetting shape.

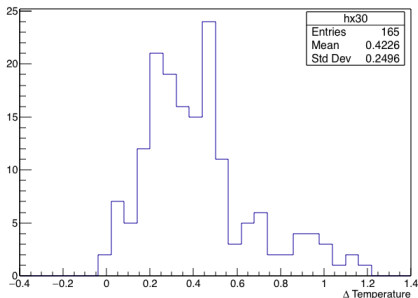


- The largest temperature difference is about 1°C .
- The central dip is the typical vignetting term.
- The increasing slope in one direction is not fully understood.

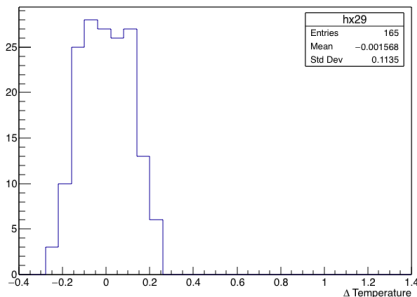


Vignetting Correction

- In an ideal case, all the squares have the same value as the central area, then the spread in average temperature is zero.



Original data.



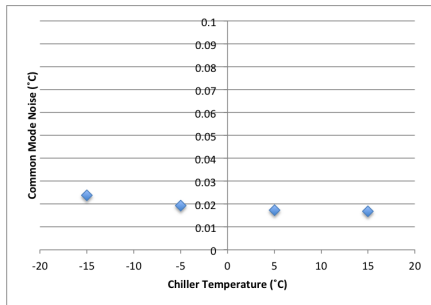
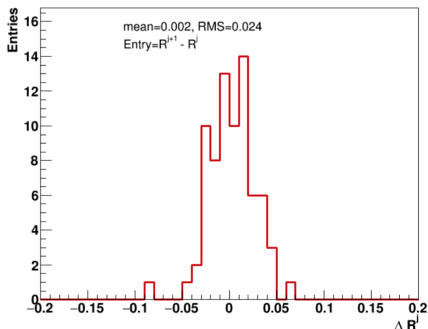
Data after correction.

- Mean moves closer to zero.
- The tail in the original data with the furthest points ($\sim 1.2^\circ\text{C}$) is corrected.
- All the areas in the FoV after the correction are within $\pm 0.2^\circ\text{C}$.



Common Mode Noise

- Common mode values cannot be determined unless T and ΔT are known.

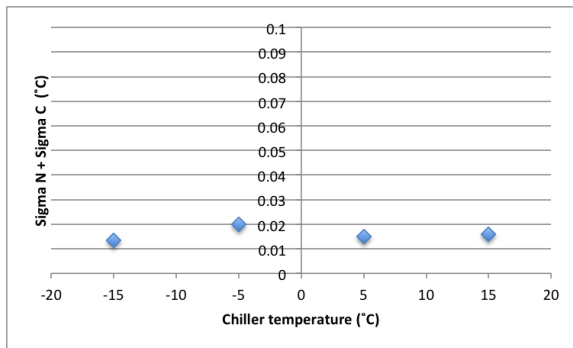


- The value of σ_C at -15°C is 0.024°C , four times smaller than the pedestal sigma.
- σ_C seems to be constant for all temperatures.



The RMS width of the raw values over many frames and pixels is given by

$$\sigma_R = \sigma_P \oplus \sigma_C \oplus \sigma_N \Rightarrow \sigma_N \oplus \sigma_C = \sigma_R \ominus \sigma_P$$



$\sigma_N \oplus \sigma_C$ are always below 0.03°C and constant in temperature.



- At the temperatures where the staves are going to be studied, all noise terms can be measured and corrected.
- Flaws in early experiments showed a delta of 2°C with respect to the pipe's temperature.
- The uncorrectable contribution for vignetting is $\pm 0.2^{\circ}\text{C}$, and $\pm 0.03^{\circ}\text{C}$ for $(\sigma_C \oplus \sigma_N)$.



The pedestal values can be determined with

$$P_i = \frac{1}{n_{\text{frame}}} \sum_{j=1}^{n_{\text{frame}}} R_i^j - \frac{1}{n_{\text{sensor}}} \sum_{i=1}^{n_{\text{sensor}}} \left(\frac{1}{n_{\text{frame}}} \sum_{j=1}^{n_{\text{frame}}} R_i^j \right).$$

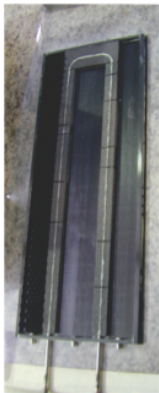
The common mode values cannot be determined unless the temperature T and temperature offset ΔT are known. However, the RMS width of the C^j distribution can be measured similarly to the P_i distribution width.

$$C_j = \frac{1}{n_{\text{sensors}}} \sum_{i=1}^{n_{\text{sensors}}} R_i^j - \frac{1}{n_{\text{frame}}} \sum_{j=1}^{n_{\text{frame}}} \left(\frac{1}{n_{\text{sensors}}} \sum_{i=1}^{n_{\text{sensors}}} R_i^j \right).$$



Missing Glue Defects

Marked missing epoxy locations



Foam epoxy mask



Missing honeycomb glue locations





Temperature Range	-40°C to 650°C
Measurement Accuracy	±2% or 2°C of reading
Field of View	25° (H) × 19° (V)
IFOV	0.68 mRad
Focus Range	25 cm to Infinity
Image Update Rate	50 frames per second
Detector	640 × 480 pixels
Spectral Band	7.5 to 14 μm
Camera Dimensions	2.9" × 3.0" × 8.5"
Camera Weight	2.98 lb

